driven by K^+ ions. However, the presence of a single 3′T appears to inhibit this process, although a residual high-temperature structure still forms in dT_4G_4T (Figure 3).

Structurally, we can say little at the moment about the remarkably stable high-temperature structure in either of these complexes in K^+. Since the CD spectrum changes in magnitude but not in shape, it seems likely that no large-scale change in geometry is involved. One possibility is that a change in hydration or ion binding occurs on heating the tetramers, but this is by no means established. Structural and thermodynamic analysis of this form of the complex is presently under way to attempt to distinguish these from other possibilities.

Registry No. dT_4G_4, 108050-57-3; dT_4G_4T, 138693-69-3; Na, 7440-23-5; K, 7440-09-7.

References

Blackburn, E. H. (1991) *Nature 350*, 569–573.

Blackburn, E. H., & Szostak, J. W. (1984) *Annu. Rev. Biochem. 53*, 163–194.

Cantor, C., Warshaw, M. W., & Shapiro, H. (1970) *Biopolymers 9*, 1059–1077.

Caruthers, M. H. (1982) in *Chemical and Enzymatic Synthesis of Gene Fragments* (Gassen, H. G., & Lang, A., Eds.) pp 71–79, Verlag Chemie, Weinheim.

Guo, Q., Lu, M., Marky, L. A., & Kallenbach, N. R. (1992) *Biochemistry* (preceding paper in this issue).

Hardin, C. C., Henderson, E., Watson, T., & Prosser, J. K. (1991) *Biochemistry 30*, 4460–4472.

Henderson, E. R., Hardin, C. C., Walk, S. K., Tinoco, I., & Blackburn, E. H. (1987) *Cell 51*, 899–908.

Henderson, E. R., Moore, M., & Malcolm, B. A. (1990) *Biochemistry 29*, 732–737.

Jin, R., Breslauer, K. J., Jones, R. A., & Gaffney, B. L. (1990) *Science 250*, 543–546.

Lipps, H. J. (1980) *Proc. Natl. Acad. Sci. U.S.A. 77*, 4104–4108.

Maxam, A., & Gilbert, W. (1980) *Methods Enzymol. 65*, 499–560.

Oka, Y., & Thomas, C. A. (1987) *Nucleic Acids Res. 15*, 8877–8898.

Sen, D., & Gilbert, W. (1988) *Nature 334*, 364–366.

Sen, D., & Gilbert, W. (1990) *Nature 344*, 410–414.

Sen, D., & Gilbert, W. (1992) *Biochemistry 31*, 65–70.

Sundquist, W. I., & Klug, A. (1989) *Nature 342*, 825–829.

Williamson, J. R., Raghuraman, M. K., & Cech, T. R. (1989) *Cell 59*, 871–880.

Zakian, V. A. (1989) *Annu. Rev. Genet. 23*, 579–604.

Zimmerman, S. B., Cohen, G. H., & Davies, D. R. (1975) *J. Mol. Biol. 92*, 181–192.

Average Density and Size of Microclusters of Epidermal Growth Factor Receptors on A431 Cells†

Paul R. St-Pierre and Nils O. Petersen*

Department of Chemistry, The University of Western Ontario, London, Ontario, Canada N6A 5B7

Received October 28, 1991; Revised Manuscript Received January 14, 1992

ABSTRACT: For some hormone receptors, the early events of signal transduction depend on their molecular arrangement and interactions at the cell surface. An understanding of the mechanism of signal transduction in general needs a careful analysis of the receptor distribution. Here, we present the first quantitative measurement of epidermal growth factor receptor distribution on A431 cells obtained by scanning fluorescence correlation spectroscopy. Prior to epidermal growth factor binding, the A431 cell membrane presents an average surface density of 7.7–8.4 microclusters/μm^2, each containing an average of 130 receptors.

There is strong evidence that the molecular organization and the lateral distribution of receptors in cell membranes are important for their function (Lichtner & Schirrmacher, 1990). In many cases, it is clear that the distribution of receptors is neither random nor homogeneous, but rather the receptors are partly aggregated (Van Belzen et al., 1988). The organization and distribution of receptors at the cell surface frequently change as a consequence of their interactions with specific hormones or ligands (Van Belzen et al., 1988; Haigler et al., 1978). Yet, some important questions about receptor distribution remain unanswered: Are receptors distributed uniformly, randomly, or among domains on the cell surface prior to the binding of hormone? If clusters exist, can their density and size be determined? What is the proportion of clustered and nonclustered receptors? What is the nature of the receptor–receptor interactions and what constraints arise from them? Answers to these and related questions will influence the way we understand the dependence of the cellular response on receptor mobility, receptor–receptor interactions, and receptor–ligand interactions. An important starting point is to measure the receptor distribution on cell surfaces *prior* to hormone binding.

The polypeptide hormone epidermal growth factor (EGF) acts through its cell surface receptor to induce cell proliferation (Schlessinger, 1986; Defize et al., 1989). Its mode of action appears to involve receptor microclustering (Schreiber et al., 1983; Yarden & Schlessinger, 1986), a mechanism thought to be common to many receptor systems. The A431 epidermoid carcinoma cell line has been used extensively in the study of the mechanism of action of the EGF receptors and is very well characterized biochemically and biophysically (Kawamoto et al., 1983; Moolenaar et al., 1987; Wiley, 1988; Roy et al., 1989; Bellot et al., 1990). Detailed analysis of the EGF-receptor organization on A431 cells has been attempted using ferritin-labeled EGF (Kawamoto et al., 1983; Mckanna et al., 1979) and monoclonal antibodies directed against the EGF receptors which are then labeled with gold-conjugated protein

† This work was supported by the Natural Sciences and Engineering Research Council of Canada.

0006-2960/92/0431-2459$03.00/0

A (Van Belzen et al., 1988; Boonstra et al., 1985) and visualized by electron microscopy techniques. Frequency distributions of cluster sizes have been calculated from the electron micrographs, where particles were defined as clustered if the distances between their centers was less than 35 nm (Van Belzen et al., 1988). Indirect evidence for receptor clusters has also been provided through measurements of rotational diffusion (Zidovetzki et al., 1981, 1986). In this case, a cluster is defined as a group of receptors being physically linked to each other such that they rotate synchronously.

Conventional fluorescence microscopy techniques provided early evidence for the active change in receptor distribution during exposure to hormone or specific ligands (Haigler et al., 1978; Schlessinger et al., 1978) but have so far failed to provide direct, quantitative information about their distribution. Attempts at quantification have come mainly from electron microscopy (Van Belzen et al., 1988; McKanna et al., 1979), but interpretation of the data is limited by inconsistent labeling efficiency. We have recently developed a new approach to measure the distribution of cell surface receptors (Petersen, 1986). Scanning fluorescence correlation spectroscopy (S-FCS) is based on number fluctuation theory (Elson & Webb, 1975) in which the average number of molecules in an open volume is related to the fluctuations in time of that number within this volume. This principle can be applied to cell membrane systems if fluctuations as a function of position on the cell surface, rather than time, are obtained by scanning an appropriately labeled cell under a laser beam of defined width. The technique provides *quantitative* measurements of the densities and sizes of receptor clusters on cell surfaces. In this case, a cluster is defined as a group of receptors whose positions are correlated through interactions but not necessarily by molecular contact. Consequently, it is possible that long-range interactions, for example, via the cytoskeleton, can provide positional correlation. In this work, we report the first quantitative and direct measurement of such clusters of EGF receptors on A431 cells.

Materials and Methods

EGF receptors were probed with mouse monoclonal IgG 29.1 antibody (Sigma Chemical Co., catalog no. E2760, lot no. 79F4816), a clone that binds uniformly to the EGF receptors independent of whether these are in a high- or a low-affinity state for the hormone EGF (Yarden et al., 1985). A431 cells (American Type Culture Collection) were fixed for 20 min at 37 °C with 0.2% paraformaldehyde prior to antibody binding to inhibit receptor internalization. This procedure does not alter the binding affinity of EGF to its receptor (Kawamoto et al., 1983). The cells were then incubated for 30 min at room temperature with a series of IgG 29.1 concentrations. The cells were rinsed and labeled for 30 min at room temperature with an FITC-conjugated goat anti-mouse Fc specific antibody (Sigma Chemical Co., catalog no. F5347, lot no. 69F4818) at a concentration of 5.6 μg/mL. Cells were mounted under the microscope objective for S-FCS experiments (St-Pierre & Petersen 1990). Briefly, a cell is translated under a focused laser beam to generate a record of fluorescence intensity as a function of position. The data are used to calculate the autocorrelation function

$$g(k\Delta x) = \frac{\frac{1}{N_k}\sum_{l=1}^{N_k} i(l\Delta x)\, i((l+k)\Delta x)}{\left(\frac{1}{N}\sum_{l=1}^{N} i(l\Delta x)\right)^2} - 1 \qquad (1)$$

where Δx is the step resolution, N is the total record length, and $N_k = N - k$. The zero-lag value $g(0)$ is calculated from a fit to the expected function

$$g(k\Delta x) = g(0)\exp(-(k\Delta x/w)^2) + g_0 \qquad (2)$$

As shown earlier (Petersen, 1986) $g(0)$ can be determined with high precision because of low noise in the $g(k\Delta x)$ function. However, because of a limited record length the accuracy of $g(0)$ for any one measurement is poorer. To get a better estimate of the true value, 30 cells are scanned under the laser beam over a distance of about 24 μm for each IgG 29.1 concentration and an average $g(0)$ value is calculated. The laser beam is focused to a width of 1.0 μm. Care was taken to obtain records over regions of the cell which are flat. This minimizes fluctuations arising from changes in the illumination intensity and detection efficiency at planes above and below the focal plane (Petersen, 1986). Computer simulations of S-FCS experiments were performed using a Fortran vectorial source code on a Cyber 2000 system. The details have been described elsewhere (St-Pierre & Petersen, 1990).

Table I: Results of S-FCS Experiments on A431 Cells

[IgG 29.1] (μg/mL)	FITC-Ab[a] (5.6 μg/mL)	$\langle i \rangle$[b] (10^3 cps)	$g(0)$	ρ_s (μm^{-2})	N[c]
0 (b)	-	4.2	0.0019		14
0 (b + n)	+	12	0.0025		18
0.0096	+	13	0.0090	0.27	19
0.096	+	30	0.0215	5.6	21
0.96	+	52	0.0267	7.3	24
3.84	+	69	0.0258	8.7	12
6.72	+	150	0.0367	7.5	23
9.6	+	61	0.0287	7.4	19

[a] FITC-conjugated goat anti-mouse Fc specific antibody. [b] cps represents counts per second. [c] Number of cells for which the autocorrelation decay is within 30% of the laser beam width.

Results

Scanning fluorescence correlation spectroscopy experiments yield (1) the average fluorescence intensity of the fluctuation record ($\langle i \rangle$), which corresponds to the actual amount of material bound to the cell surface, and (2) the variance in the amplitude of the fluctuations $g(0)$, which is inversely proportional to the density of independently distributed fluorescent entities. Typical examples of fluorescence scans and their corresponding correlation functions are shown in Figure 1 for low and high concentrations of IgG 29.1 antibodies. The results of many such measurements, at concentrations ranging over 3 orders of magnitude, are summarized in Table I, along with the corresponding control experiments conducted without primary antibody. It is clear that the $g(0)$ values, representing the density of receptor entities, become independent of primary antibody concentration. We have previously shown that the concentration independence of $g(0)$ is characteristic of partly or completely aggregated receptor systems (Petersen, 1986; St-Pierre & Petersen, 1990). This is because an increase in the number of receptors labeled within an aggregate does not change the number of aggregates; they only become brighter.

Previous work shows that computer simulations of scanning fluorescence correlation spectroscopy experiments provide a useful approach to determine the detailed receptor distribution (St-Pierre & Petersen, 1990). For example, data obtained from experiments detecting concanavalin A receptor distribution on mouse fibroblasts have been modeled successfully by computer simulations which incorporate two distinct receptor populations: one with a few very large clusters and the other with many small clusters. These simulations also show that the concanavalin A concentration dependence of $g(0)$ is recovered only if large and small receptor clusters are asso-

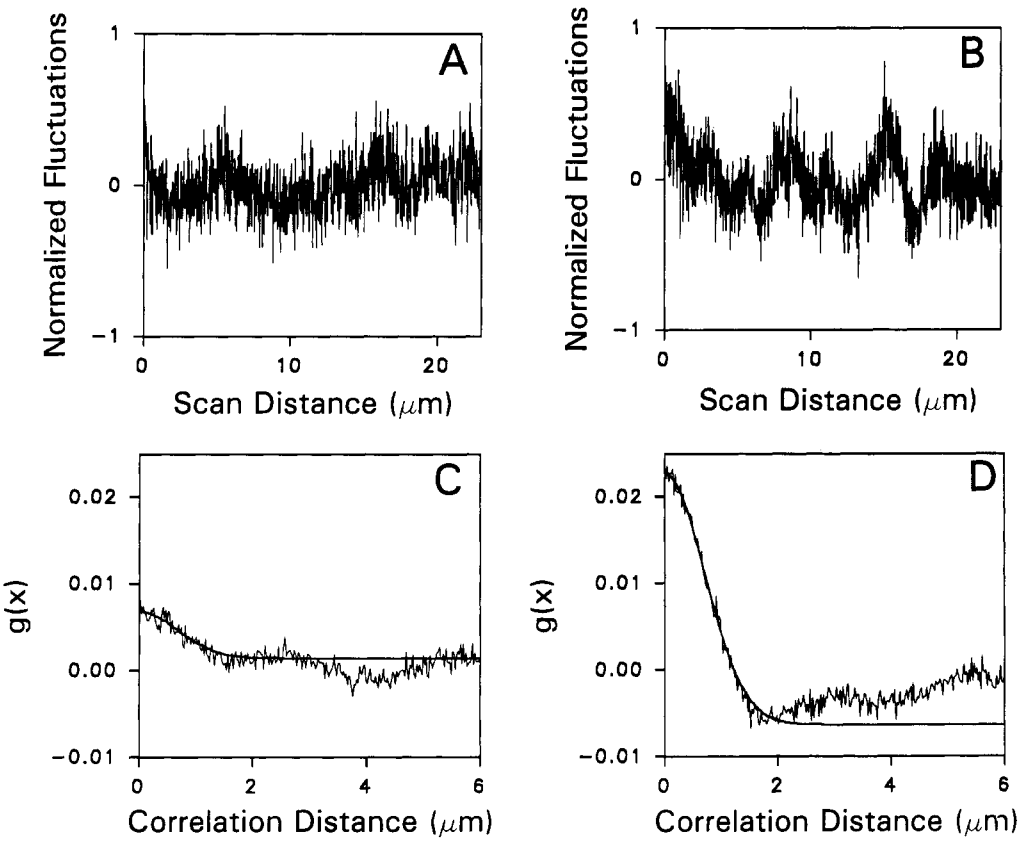

FIGURE 1: Samples of fluorescence scans (A, B) and corresponding autocorrelation functions (C, D) at 0.0096 μg mL^{-1} (A, C) and 9.6 μg mL^{-1} (B, D) IgG 29.1 antibody. The normalized fluctuations were calculated as $[i - \langle i \rangle]/\langle i \rangle$. The $g(0)$ value is derived from the fit to the correlation function, allowing for the variation in the base-line level. The laser beam width of 1.0 ± 0.2 μm is reproduced by the autocorrelation functions.

ciated respectively with the low- and high-affinity classes of binding sites, known to exist for concanavalin A receptors.

In the present work, computer simulations are designed with two variables: the density of points (labeled receptor clusters) positioned randomly on a flat surface (the cell) and the weight of each point (as a measure of the amount of label). The points within a circle of defined radius (the laser beam) are added according to their weight and position to give a single count (intensity). The count records obtained by translating the circle across the surface are analogous to the experimental fluorescence intensity records (Figure 1A,B). To get an average simulated $g(0)$ value, many count records are generated with different point positions at fixed density and weight. Systematic variation of the weight of the points for a fixed density permits simulation of changes in labeling. Figure 2 compares the experimental $g(0)$ values as a function of the average fluorescence intensity with simulated $g(0)$ values obtained with a density of evenly weighted points set at 8.4/μm^2.

The complete simulation of the experimental $g(0)$ for fluorescently labeled cell surfaces requires two other point populations representing the cell background fluorescence and the nonspecific binding of the secondary antibody. These latter point-population densities and weights were calculated (Table II) from the experimentally observed values for the unlabeled cells and the nonspecifically labeled cells (Table I, control experiments without IgG 29.1) and were included in the above simulations. The simulated $g(0)$ values and average weights (intensity) for both control experiments correspond very well to the experimentally observed values as shown by the overlap of the first two points in Figure 2.

An alternative to direct simulations is to correct the raw data for contributions from the cell background (b) and nonspecifically bound secondary antibodies (n). The advantage of this method is that the density of the specifically bound antibody emerges directly from the corrected data. The fluctuation information from the specifically bound secondary

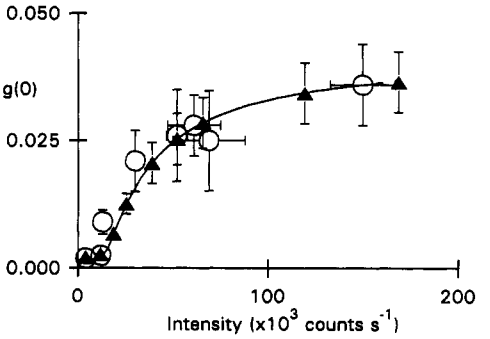

FIGURE 2: Zero-lag value of the photocurrent autocorrelation function $g(0)$ measured on A431 cells (○) and on simulated cell surfaces (▲) as a function of average fluorescence intensities. Each simulated data point represents an average of 20 records. The error bars represent the standard error of the mean values calculated with a 95% level of confidence.

Table II: Parameters Used in Computer Simulations[a]

point distribution	density (μm^{-2})	wt
background (b)	168	16
secondary Ab (n)	59.3	84
clusters (s)	8.43	11100[b]

[a] The corresponding $g(0)$ values and average counts are plotted in Figure 1. [b] This value is the weight that the points (clusters) must have to give records with an average count corresponding to the largest average fluorescence intensity of the experimental data, where receptor saturation is assumed. Division by 84 gives a cluster size of 132.

antibodies (s) can be retrieved by

$$g_s(0) = \langle i \rangle_s^{-2}[g(0)\langle i \rangle^2 - g_{b+n}(0)\langle i \rangle_{b+n}^2] \quad (3)$$

where

$$\langle i \rangle_s = \langle i \rangle - \langle i \rangle_{b+n} \quad (4)$$

This approximation is valid only if the variances in the amplitude of fluctuations of each source of fluorescence are statistically independent. Since $1/g_s(0)$ is proportional to the average number of clusters in the illuminated area of the cell membrane, the surface density of the labeled EGF-receptor clusters is $\rho_s = [g_s(0)\pi w^2]^{-1}$, where w is the laser beam width. The surface density values (ρ_s) are calculated and shown in Table I for each experiment. The surface density is small at low primary antibody concentrations and increases steeply, indicating that more clusters are being detected. The surface density then levels off at high concentrations because the same number of clusters per square micrometer are being counted despite the further labeling. The average density determined at the plateau corresponds to 7.7 clusters/μm^2.

Both approaches confirm that a model in which EGF receptors are distributed at the surface of A431 cells as a population of homogeneous clusters is adequate and appropriate. The average cluster density for the EGF receptor is 7.7–8.4 clusters/μm^2.

The average size of the EGF-receptor clusters may be estimated from the maximum number of labeled antibodies which can bind to them. Assuming that the maximum average fluorescence intensity found in Table I represents the saturating condition, the corresponding weight of the points in the simulations can be divided by the corresponding weight of a single fluorescently labeled secondary antibody given by the control experiments (Table II). This calculation gives a maximum of about 130 fluorescent antibodies bound per EGF-receptor cluster.

Surface folds or microvilli do not contribute significantly to the cluster measurements since the density measured with nonspecific labeling is much greater than that with receptor labeling (Table II). If these surface convolutions were of primary importance, the density observed by uniform nonspecific labeling of the cell should be the same as that of the receptors, in the present case around 8/μm^2.

Discussion

Two lines of argument suggest that the maximum number of secondary antibodies bound to IgG 29.1 is equal to the number of receptors per cluster. First, the primary antibody is a mouse monoclonal antibody directed at a single antigenic site on the carbohydrate moiety of the EGF receptor (Defize et al., 1987). Thus we expect at most one IgG 29.1 per receptor. The secondary antibody is a FITC-labeled goat antibody directed specifically at the F_c portion of mouse antibodies. Therefore, it is reasonable that the secondary antibody binds to one IgG 29.1 antibody, preserving a one-to-one ratio with the EGF receptor. Second, the measured value of 130 receptors per cluster with 7.7–8.4 clusters/μm^2 yields a total receptor density of about 1000–1100 receptors/μm^2. This compares well with the estimate of 700–1100 receptors/μm^2 derived from using (2–3) $\times 10^6$ receptors per A431 cell (Kawamoto et al., 1983), for which an average surface area of 2800 μm^2 was determined (Haigler et al., 1979).

The agreement between our total receptor density and that measured by others lends credence to the distribution analysis and establishes that the distribution is representative of all the EGF receptors on A431 cells. The receptor distribution measured here is, however, different than that measured by others (Van belzen et al., 1988; Haigler et al., 1979; McKanna et al., 1979; Boonstra et al., 1985; Zidovetzki et al., 1981). There is no direct evidence for a substantial number of dimers and trimers as indicated by electron microscopy. Our data are more consistent with the slowly rotating receptor population inferred by rotational diffusion measurements although the clusters contain at least four times more receptors.

S-FCS does not provide direct evidence of the physical dimension of the receptor clusters. The upper limit is about 200 nm in diameter because clusters larger than 1% of the laser beam area would cause detectable distortions of the autocorrelation function (Abney et al., 1990). A lower limit of 80 nm in diameter corresponds to the dimension of a compact cluster of 130 receptors. These dimensions are comparable to the diameter of 120 nm found for cytoplasmic vesicles containing EGF receptors detected by electron microscopy on A431 cells after a short incubation with ferritin–EGF (Haigler et al., 1979). In contrast, the density and dimension of coated pits are not compatible with the domains measured here (Anderson et al., 1976). The present experimental data reveal the average density and size of the domains within which the receptors are confined in a correlated manner. Our experiments do not provide insight into how this correlation arises and do not exclude the existence of dimers and trimers within the domains.

Fluorescence photobleaching measurements clearly show that about 60% of the EGF receptors are mobile on the surface of A431 cells with a diffusion coefficient of 8.5×10^{-10} cm^2 s^{-1} (Hillman & Schlessinger, 1982). The large mobile population measured by Hillman and Schlessinger *must* be compatible with the receptor distribution derived from our data. Consequently, the individual units of mobile receptors must reside most of the time within the domains, since our data account for all of the receptors. This apparent contradiction of mobile, yet clustered, receptors is only resolved if the majority of the EGF receptors can exchange rapidly among the immobile domains, thereby allowing for long-distance mobility. For a model of rapid exchange between immobile domains, the observed diffusion coefficient is the product of the instantaneous fraction of mobile receptors and the theoretical diffusion coefficient (Elson & Reidler, 1979). For the EGF-receptor system the measured diffusion coefficient and that calculated as 3×10^{-8} cm^2 s^{-1} (Peters & Cherry, 1982) indicate that no more than 2% of all receptors are moving freely at any given time outside the domains. This small fraction is consistent with the receptor distribution measured here. The mean free path for movement of an individual receptor between domains is inversely proportional to the domain density and diameter (McQuarrie, 1976). With the present data, we calculate a mean free path between 3 and 16 μm. These distances are in agreement with recent measurements of movement of gold particles attached to receptors (Sheetz et al., 1990) (albeit not EGF receptors). This movement may be a direct observation of mobility within domains coupled with fast exchange between domains.

Our results provide important quantitative information about the EGF-receptor distribution. It is suggested that the receptors are distributed at the surface of A431 cells *prior* to EGF binding in a domain-like configuration at a density of about 8/μm^2. Each domain contains an average of 130 receptors. We also conclude that the majority of the receptors must be diffusing in the cell membrane via a mechanism of fast exchange between domains. Finally, these results should be useful in calculations of the rate of binding of the hormone to the receptor (De Meyts, 1976; Delisi, 1980; Van Opheusden

et al., 1984; Zheng & Chiew, 1990) as well as in considerations of the dynamics of interactions among receptors (Levitzki & Schlessinger, 1974; Meakin, 1985) or between receptors and the cytoskeleton (Jacobson, 1983).

Registry No. EGF, 62229-50-9.

REFERENCES

Abney, J. R., Scalettar, B. A., & Hackenbrock, C. R. (1990) *Biophys. J. 58*, 261–265.

Anderson, R. G. W., Goldstein, J. L., & Brown, M. S. (1976) *Proc. Natl. Acad. Sci. U.S.A. 73*, 2434–2438.

Bellot, F., Moolenaar, W., Kris, R., Mirakhur, B., Verlaan, I., Ullrich, A., Schlessinger, J., & Felder, S. (1990) *J. Cell Biol. 110*, 491–502.

Boonstra, J., van Maurik, P., Defize, L. H. K., de Laat, S. W., Leunissen, J. L. M., & Verkley, A. J. (1985) *Eur. J. Cell Biol. 36*, 209–216.

Defize, L. H. K., Mummery, C. L., Moolenaar, W. H., & de Laat, S. W. (1987) *Cell Differ. 20*, 87–102.

Defize, L. H. K., Boonstra, J., Meisenhelder, J., Kruijer, W., Tertoolen, L. G. J., Tilly, B. C., Hunter, T., van Bergen en Henegouwen, P. M. P., Moolenaar, W. H., & de Laat, S. W. (1989) *J. Cell Biol. 109*, 2495–2507.

DeLisi, C. (1980) *Q. Rev. Biophys. 13*, 201–230.

De Meyts, P. (1976) *J. Supramol. Struct. 4*, 241–258.

Elson, E. L., & Webb, W. W. (1975) *Annu. Rev. Biophys. Bioeng. 4*, 311–334.

Elson, E. L., & Reidler, J. A. (1979) *J. Supramol. Struct. 12*, 481–489.

Haigler, H., Ash, J. F., Singer, S. J., & Cohen, S. (1978) *Proc. Natl. Acad. Sci. U.S.A. 75*, 3317–3321.

Haigler, H. T., McKanna, J. A., & Cohen, S. (1979) *J. Cell Biol. 81*, 382–395.

Hillman, G. M., & Schlessinger, J. (1982) *Biochemistry 21*, 1667–1672.

Jacobson, B. S. (1983) *Tissue Cell 15*, 829–852.

Kawamoto, T., Sato, J. D., Le, A., Polikoff, J., Sato, G. H., & Mendelsohn, J. (1983) *Proc. Natl. Acad. Sci. U.S.A. 80*, 1337–1341.

Levitzki, A., & Schlessinger, J. (1974) *Biochemistry 13*, 5214–5219.

Lichtner, R. S., & Schirrmacher, V. (1990) *J. Cell. Physiol. 144*, 303–312.

McKanna, J. A., Haigler, H. T., & Cohen, S. (1979) *Proc. Natl. Acad. Sci. U.S.A. 76*, 5689–5693.

McQuarrie, D. A. (1976) in *Statistical Mechanics* (Harper & Row, Eds.) pp 358–359, Harper Collins, New York, NY.

Meakin, P. (1988) in *Phase transitions and critical phenomena* (Domb, C., & Lebowitz, J. L., Eds.) pp 335–489, Academic Press, San Diego, CA.

Moolenaar, W. H., Defize, L. H. K., Tilly, B. C., Bierman, A. J., & de Laat, S. W. (1987) in *Hormones and cell regulation* (Dummont, J. E., & Nunez, J., Eds.) pp 145–152, Elsevier/North-Holland Biomedical Press, New York, NY.

Peters, R., & Cherry, R. J. (1982) *Proc. Natl. Acad. Sci. U.S.A. 79*, 4317–4321.

Petersen, N. O. (1986) *Biophys. J. 49*, 809–815.

Roy, L. M., Gittinger, C. K., & Landreth, G. E. (1989) *J. Cell. Physiol. 140*, 295–304.

Schlessinger, J. (1986) in *Oncogenes and growth control* (Kahn, P., & Graf, T., Eds.) pp 77–84, Springer-Verlag, New York, NY.

Schlessinger, J., Shechter, Y., Willingha, M. C., & Pastan, I. (1978) *Proc. Natl. Acad. Sci. U.S.A. 75*, 2659–2663.

Schreiber, A. B., Libermann, T. A., Lax, I., Yarden, Y., & Schlessinger, J. (1983) *J. Biol. Chem. 258*, 846–853.

Sheetz, M. P., Baumrind, N. L., Wayne, D. B., & Pearlman, A. L. (1990) *Cell 61*, 231–241.

St-Pierre, P. R., & Petersen, N. O. (1990) *Biophys. J. 58*, 503–511.

Van Belzen, N., Rijken, P. J., Hage, W. J., de Laat, S. W., Verkleij, A. J., & Boonstra, J. (1988) *J. Cell. Physiol. 134*, 413–420.

van Opheusden, J. H. J., Wiegel, F. W., & Goldstein, B. (1984) *Biophys. Chem. 20*, 237–248.

Wiley, H. S. (1988) *J. Cell Biol. 107*, 801–810.

Yarden, Y., & Schlessinger, J. (1986) *ICSU Short Rep. 4*, 164–171.

Yarden, Y., Harari, H., & Schlessinger, J. (1985) *J. Biol. Chem. 260*, 315–319.

Zheng, L., & Chiew, Y. C. (1990) *J. Chem. Phys. 93*, 2658–2663.

Zidovetzki, R., Yarden, Y., Schlessinger, J., & Jovin, T. M. (1981) *Proc. Natl. Acad. Sci. U.S.A. 78*, 6981–6985.

Zidovetzki, R., Yarden, Y., Schlessinger, J., & Jovin, T. M. (1986) *EMBO J. 5*, 247–250.